

## NOT STRANGE BUT BIZARRE PHYSICS FROM THE SAMPLE EXPERIMENT

DEREK B. LEINWEBER

*Department of Physics and Math. Physics, University of Adelaide 5005, Australia*

*E-mail: dleinweb@physics.adelaide.edu.au*

Since the report of the SAMPLE Collaboration suggesting the strange-quark contribution to the nucleon,  $G_M^s(0)$ , may be greater than zero, numerous models have appeared supporting positive values for  $G_M^s(0)$ . In this paper the bizarre physics associated with  $G_M^s(0) > 0$  is illustrated. Using new lattice QCD results, our best estimate for  $G_M^s(0)$  shifts slightly from  $G_M^s(0) = -0.75 \pm 0.30 \mu_N$ , to  $G_M^s(0) = -0.62 \pm 0.26 \mu_N$ .

### 1 Introduction

A report of the first experimental measurement of the strange-quark contribution to the nucleon magnetic moment,  $G_M^s(0)$ , was recently published by the SAMPLE collaboration<sup>1</sup>. Their findings indicate

$$G_M^s(0.1 \text{ GeV}^2) = +0.23 \pm 0.37 \pm 0.15 \pm 0.19 \mu_N, \quad (1)$$

where the uncertainties are of statistical, systematic, and theoretical origin respectively.<sup>a</sup> While the uncertainties of the measurement are somewhat large and certainly include negative values, this result suggests that  $G_M^s(0)$  may actually be positive. Since the appearance of the SAMPLE result<sup>1</sup>, numerous papers have appeared suggesting  $G_M^s(0) > 0$ . It is the purpose of this discussion to point out the bizarre properties of QCD that must be true if  $G_M^s(0) > 0$ , and illustrate why future experiments are more likely to find a large negative value closer to  $G_M^s(0) \sim -0.6 \mu_N$ .

The Euclidean path integral formulation of quantum field theory is the origin of fundamental approaches to the study of quantum chromodynamics (QCD) in the nonperturbative regime. An examination of the symmetries manifest in the QCD path integral for current matrix elements reveals various relationships among the quark sector contributions<sup>2</sup>. These relationships are sufficient to express the strange-quark contribution to the nucleon magnetic moment,  $G_M^s(0)$ , in terms of the experimentally measured baryon magnetic

---

Presented at the workshop on "Future Directions in Quark Nuclear Physics," CSSM, Adelaide, March 9-20, 1998. This and related papers may be obtained from:

<http://www.physics.adelaide.edu.au/theory/staff/leinweber/publications.html>

<sup>a</sup>The charge of the strange-quark is not included in the definition of  $G_M^s(0)$ .

moments of  $p$ ,  $n$ ,  $\Sigma^+$ ,  $\Sigma^-$ ,  $\Xi^0$  and  $\Xi^-$ , and two ratios of quark-sector contributions to magnetic moments. These quark-sector ratios include the  $s/d$  sea-quark loop ratio, and either the  $u_p/u_{\Sigma^+}$  ratio, expressing the difference between a valence  $u$ -quark contribution to the proton and the analogous contribution when the  $u$ -quark resides in the  $\Sigma$  baryon, or the  $u_n/u_{\Xi^0}$  ratio expressing the contribution of a valence  $u$ -quark to the neutron relative to that when the  $u$  quark resides in  $\Xi^0$ . In simple models, the  $s/d$  sea-quark loop ratio is given by a ratio of constituent quark masses<sup>2</sup>  $\sim 0.65$  while the valence ratios are assumed to be 1.

## 2 Valence Versus Sea Quarks

Here we carefully illustrate what is meant by sea-quark-loop contributions and valence-quark contributions. Finally, the expressions for  $G_M^s(0)$  are presented.

Current matrix elements of hadrons are extracted from the three-point function, a time-ordered product of three operators. Generally, an operator exciting the hadron of interest from the QCD vacuum is followed by the current of interest, which in turn is followed by an operator annihilating the hadron back to the QCD vacuum.

In calculating the three point function, one encounters two topologically different ways of performing the current insertion. Figure 1 displays skeleton diagrams for these two insertions. These diagrams may be dressed with an arbitrary number of gluons. The left diagram illustrates the connected insertion of the current to one of the valence<sup>b</sup> quarks of the baryon. It is here that Pauli-blocking in the sea contributions is taken into account. The right-hand diagram accounts for the alternative time ordering where the probing current first produces a  $q\bar{q}$  pair which in turn interacts with the valence quarks of the baryon via gluons.

The symmetry of the three-point correlation functions for octet baryons having two identical quark flavors, provides the following equalities for electromagnetic current matrix elements<sup>2</sup>

$$\begin{aligned} p &= e_u D_N + e_d S_N + O_N, & n &= e_d D_N + e_u S_N + O_N, \\ \Sigma^+ &= e_u D_\Sigma + e_s S_\Sigma + O_\Sigma, & \Sigma^- &= e_d D_\Sigma + e_s S_\Sigma + O_\Sigma, \\ \Xi^0 &= e_s D_\Xi + e_u S_\Xi + O_\Xi, & \Xi^- &= e_s D_\Xi + e_d S_\Xi + O_\Xi. \end{aligned} \quad (2)$$

---

<sup>b</sup>Note that the term “valence” used here differs with that commonly used surrounding discussions of deep-inelastic structure functions. Here “valence” simply describes the quark whose quark flow line runs continuously from  $0 \rightarrow x_2$ . These lines can flow backwards as well as forwards in time and therefore have a sea contribution associated with them<sup>3</sup>.

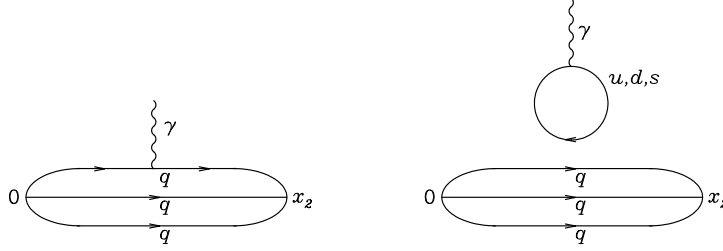


Figure 1: Diagrams illustrating the two topologically different insertions of the current. These skeleton diagrams for the connected (left) and disconnected (right) current insertions may be dressed by an arbitrary number of gluons.

Here,  $D$ ,  $S$ , and  $O$  represent contributions from the doubly represented valence-quark flavor, the singly represented valence flavor, and the sea-quark-loop sector depicted in the right-hand drawing of Fig. 1 respectively. The baryon label represents the magnetic moment. Subscripts allow for environment sensitivity explicit in the three-point function<sup>2</sup>. For example, the three-point function for  $\Sigma^+$  is the same as for the proton, but with  $d \rightarrow s$ . Hence, a  $u$ -quark propagator in  $\Sigma^+$  is multiplied by an  $s$ -quark propagator, whereas in the proton the  $u$ -quark propagators are multiplied by a  $d$ -quark propagator. The different mass of the neighboring quark gives rise to an environment sensitivity in the  $u$ -quark contributions to observables<sup>2,4,5,6,7,8,9</sup>. This point sharply contrasts the concept of an intrinsic-quark property which is independent of the quark's environment.

Focusing now on the nucleon, we note that for magnetic properties,  $O_N$  contains sea-quark-loop contributions from primarily  $u$ ,  $d$ , and  $s$  quarks. In the  $SU(3)$ -flavor limit the charges add to zero and the sum vanishes. However, the heavier strange quark mass allows for a nontrivial result. By definition

$$O_N = \frac{2}{3} {}^\ell G_M^u - \frac{1}{3} {}^\ell G_M^d - \frac{1}{3} {}^\ell G_M^s, \quad (3)$$

$$= \frac{{}^\ell G_M^s}{3} \left( \frac{1 - {}^\ell R_d^s}{{}^\ell R_d^s} \right), \quad \text{where} \quad {}^\ell R_d^s \equiv \frac{{}^\ell G_M^s}{{}^\ell G_M^d}, \quad (4)$$

and the leading superscript  $\ell$  reminds the reader that the contributions are loop contributions. Note that  ${}^\ell G_M^u = {}^\ell G_M^d$  when  $m_u = m_d$ . In the simple quark model  ${}^\ell R_d^s = m_d/m_s \simeq 0.65$ . However, we will consider  ${}^\ell R_d^s$  in the range  $-2$  to  $2$ .

With no more than a little accounting, the disconnected sea-quark-loop contributions to the nucleon,  $O_N$  may be isolated from (2) in the following two

favorable forms,

$$O_N = \frac{1}{3} \left\{ 2p + n - \frac{D_N}{D_\Sigma} (\Sigma^+ - \Sigma^-) \right\}, \quad (5)$$

$$O_N = \frac{1}{3} \left\{ p + 2n - \frac{S_N}{S_\Xi} (\Xi^0 - \Xi^-) \right\}. \quad (6)$$

In terms of valence-quark flavors,  $D_N/D_\Sigma = u_p/u_\Sigma \equiv d_n/d_\Sigma$  and  $S_N/S_\Xi = d_p/d_\Xi \equiv u_n/u_\Xi$ . In many quark models, these ratios are simply taken to be one. However, we will consider the range 0 to 2. Equating (4) with (5) or (6) provides

$$G_M^s = \left( \frac{\ell R_d^s}{1 - \ell R_d^s} \right) \left[ 2p + n - \frac{u_p}{u_{\Sigma^+}} (\Sigma^+ - \Sigma^-) \right], \quad (7)$$

and

$$G_M^s = \left( \frac{\ell R_d^s}{1 - \ell R_d^s} \right) \left[ p + 2n - \frac{u_n}{u_{\Xi^0}} (\Xi^0 - \Xi^-) \right]. \quad (8)$$

Incorporating the experimentally measured baryon moments indicates

$$G_M^s = \left( \frac{\ell R_d^s}{1 - \ell R_d^s} \right) \left[ 3.673 - \frac{u_p}{u_{\Sigma^+}} (3.618) \right], \quad (9)$$

and

$$G_M^s = \left( \frac{\ell R_d^s}{1 - \ell R_d^s} \right) \left[ -1.033 - \frac{u_n}{u_{\Xi^0}} (-0.599) \right], \quad (10)$$

where the moments are in units of nuclear magnetons ( $\mu_N$ ). These expressions for  $G_M^s(0)$  are perfectly valid for equal  $u$  and  $d$  current-quark masses and involve no other approximations. Equation (10) provides a particularly favorable case for the determination of  $G_M^s$  with minimal dependence on the valence-quark ratio. In this short discussion, we will focus on (10) alone. A discussion of (9) will appear in a more comprehensive publication<sup>10</sup>.

### 3 Bizarre Properties

Here we illustrate the bizarre properties of QCD that must be true if  $G_M^s(0) > 0$ . Moreover, we'll see how a large negative strange-quark moment the order of<sup>2</sup>  $G_M^s = -0.75 \mu_N$  provides results more in accord with our understanding of the properties of QCD.

Defining  $G_M^s(0)$  in terms of two quark-sector ratios allows one to plot the surface for  $G_M^s(0)$  and study its properties as a function of the quark-sector ratios. Figure 2 illustrates the surface for  $G_M^s(0)$  based on (10).

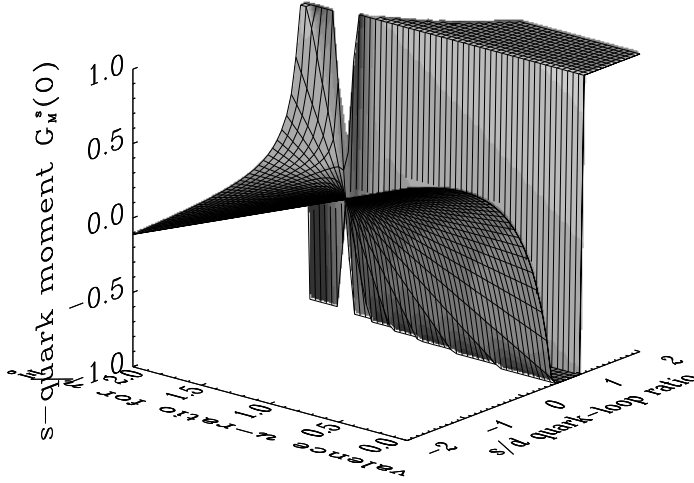


Figure 2: The surface for  $G_M^s(0)$  determined by equation (10).

Since the  $s$  quark is heavier than the  $d$  quark, it would be very unusual to find an enhancement in the  $s$ -quark-loop moment relative to the  $d$ -quark-loop moment. Such an occurrence would place the loop-ratio  $^\ell R_d^s$  greater than one. Likewise, the mass effect is not expected to change the sign of the  $s$ -quark-loop moment relative to the  $d$ -quark-loop moment, but rather simply suppress the  $s$ -quark-loop moment relative to the  $d$ -quark-loop moment. Hence, the region of interest along the  $s/d$  quark-loop ratio axis is the range  $0 \rightarrow 1$ , and it would be bizarre to find the ratio outside of this range.

Similarly, the ratio of valence  $u$ -quark moments depending on whether the  $u$  quark is in an environment of two  $d$  quarks or two  $s$  quarks,  $u_n/u_\Xi$ , is expected to be the order of one. It is important to understand that this is a secondary effect in the total baryon magnetic moment. The main difference between the  $n$  and  $\Xi^0$  magnetic moments is the difference between the magnetic moment contributions of  $s$  versus  $d$  quarks.

Figure 3 illustrates the surface of (10) where  $G_M^s(0) \geq 0$ . We see that the solution of (10) for the sea-quark-loop ratio in the region  $0 \rightarrow 1$  requires rather large values for the valence-quark moment ratio  $u_N/u_\Xi > 1.7$ . To assess whether such a ratio is reasonable, we turn to ratios of the baryon masses and to best estimates from lattice QCD.

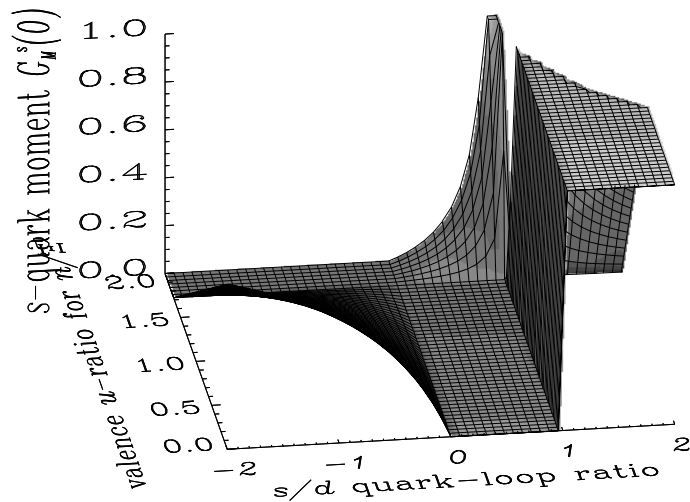


Figure 3: The surface for  $G_M^s(0) \geq 0$  determined by equation (10).

Figure 4 displays the intersection of Figure 3 and a horizontal plane at the experimental central value of  $G_M^s(0) = +0.23$ . As such, it maps out the relationship between the two quark-moment ratios which reproduces the experimental result. This relationship is indicated by the two curves in the upper-right and lower-left.

The upper region filled by backward slashes is the region between the baryon-mass ratios  $M_n/M_\Xi$  and  $M_\Xi/M_n$ . These mass ratios reflect the direct effect of the strange quark mass in much the same way as the quark-moment ratio  $d_n/s_\Xi$ . Such an effect is expected to be much larger than the secondary effect of a change in the environment probed by  $u_n/u_\Xi$ . Still the mass-ratio region fails to intersect with the positive  $G_M^s(0)$  preferred by the SAMPLE result when  ${}^\ell R_d^s > 0$ .

To further explore the  $u_n/u_\Xi$  ratio suggested by the SAMPLE result, we turn to the best lattice QCD calculations of environment sensitivity for these moments<sup>4,6</sup>. Because of the nature of the ratios involved, the systematic uncertainties in the lattice QCD calculations are expected to be small relative to the statistical uncertainties. The lattice-QCD result of  $u_n/u_\Xi = 0.72 \pm 0.46$  is illustrated in Figure 4 by the lower forward-slash filled region. This result suggests that the ratio is most likely less than 1 and makes the large values

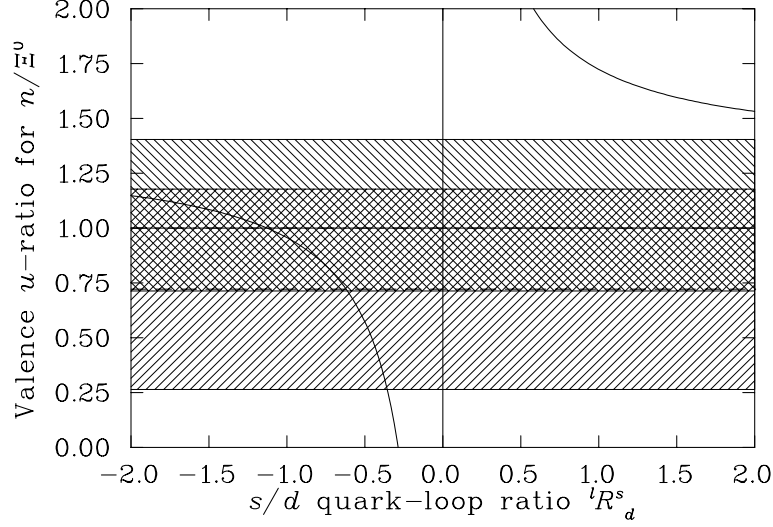


Figure 4: The intersection of Figure 3 and a horizontal plane at the central experimental value of  $G_M^s(0) = +0.23$ . Shaded regions are described in the text.

required to stay in the region of interest for the sea-quark-loop ratio look unusual.

To contrast the bizarre physics associated with a positive value for  $G_M^s(0)$  we illustrate the surface of (10) where  $G_M^s(0) \leq 0$  in Figure 5. Here we see it is easy to satisfy the expected properties of QCD.

Figure 6 displays the intersection of Figure 5 and a horizontal plane at  $G_M^s(0) = -0.75$ . The curve maps out the relationship between the two quark-moment ratios which reproduces this large negative result for  $G_M^s(0)$ . The shaded regions discussed earlier have plenty of overlap with the regions  $0 < \ell R_d^s < 1$  and  $u_n/u_{\Xi} \sim 1$ . Figure 7 provides a detailed view of the surface for  $-1 \leq G_M^s(0) \leq 0 \mu_N$  in the region of interest.

#### 4 Summary Remarks and Outlook

We have presented two equations describing the strange quark contribution to the nucleon magnetic moment  $G_M^s(0)$  in terms of the ratio of strange to light sea-quark-loop contributions and valence-quark ratios probing the subtle effects of environment sensitivity. The equations involve no approximations outside of the usual assumption of equal current quark masses. The sea-quark-

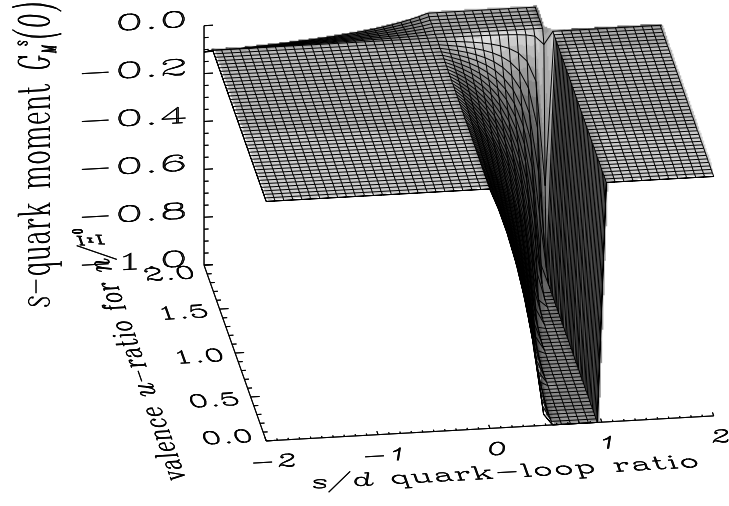


Figure 5: The surface for  $-1 \leq G_M^s(0) \leq 0 \mu_N$  determined by equation (10).

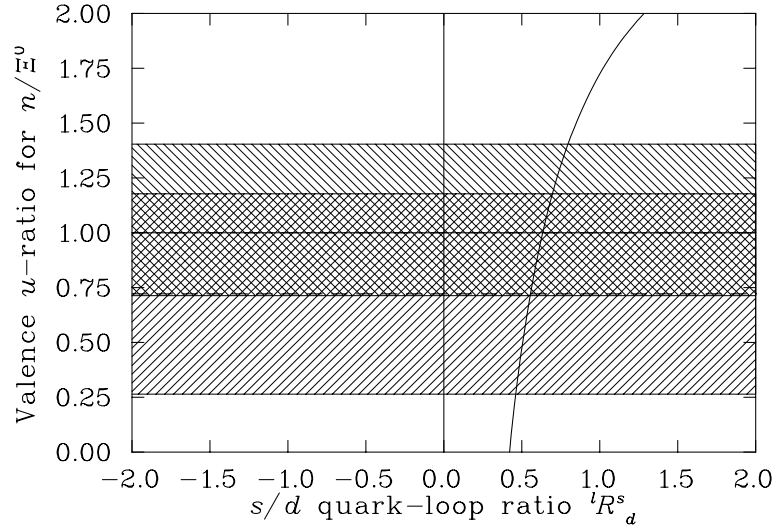


Figure 6: The intersection of Figure 5 and a horizontal plane at the previously estimated value of  ${}^2G_M^s(0) = -0.75$ . Shaded regions are described in the text.



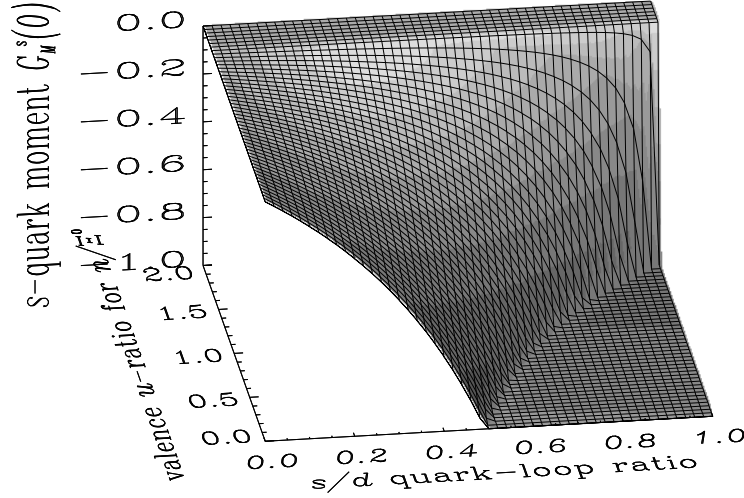


Figure 7: A detailed view of the surface for  $-1 \leq G_M^s(0) \leq 0 \mu_N$  from equation (10) in the region of interest.

loop ratio probes the quark-mass suppression of the strange-quark loop relative to the light-quark loop such that the ratio is expected to lie between 0 and 1. Best estimates<sup>11</sup> place the ratio<sup>c</sup> at  $0.55(6)$ . The valence-quark ratios probing the effects of environment sensitivity are expected to be the order of 1. Estimates based on SU(3) flavor symmetry breaking in the baryon masses and lattice QCD indicate that valid solutions require  $G_M^s(0)$  large and negative.

Positive values for  $G_M^s(0)$  require the sea-quark-loop ratio to exhibit bizarre behavior by having either the heavier quark mass enhance the magnetic moment contribution or have the mass effect actually change the sign of the sea-quark magnetic-moment contribution. Alternatively, the valence-quark ratio  $u_n/u_\Xi$  probing environment sensitivity is required to be much larger than 1 and larger than conservative limits.

Using the lattice-QCD result<sup>4,6</sup> of  $u_n/u_\Xi = 0.72 \pm 0.46$  and the new direct lattice-QCD estimation<sup>11</sup> for the sea-quark-loop ratio  ${}^\ell R_d^s = 0.55 \pm 0.06$ , our

<sup>c</sup>Jackknife errors are not available for this ratio. The quoted uncertainties are based on a correlated relative-error analysis where  $y = a/b$  and  $dy/y = |da/a - db/b|$ . This approach is known to reproduce uncertainties for closely related ratios<sup>11</sup> where jackknife error estimates have been performed.

best estimate shifts slightly from <sup>2</sup>  $G_M^s(0) = -0.75 \pm 0.30 \mu_N$ , to

$$G_M^s(0) = -0.62 \pm 0.26 \mu_N . \quad (11)$$

### Acknowledgements

I thank Tony Thomas and Tony Williams for insightful conversations. Support from the Australian Research Council is also gratefully acknowledged.

### References

1. SAMPLE Collaboration (B. Mueller, *et al.*). *Phys. Rev. Lett.* , 78:3824, 1997. nucl-ex/9702004.
2. D. B. Leinweber. *Phys. Rev.* , D53:5115, 1996. hep-ph/9512319.
3. T. D. Cohen and D. B. Leinweber. *Comments Nucl. Part. Phys.* , 21:137, 1993.
4. D. B. Leinweber, R. M. Woloshyn, and T. Draper. *Phys. Rev. D*, 43:1659, 1991.
5. D. B. Leinweber. *Phys. Rev. D*, 45:252, 1992.
6. D. B. Leinweber, T. Draper, and R. M. Woloshyn. *Phys. Rev. D*, 46:3067, 1992.
7. D. B. Leinweber. *Phys. Rev. D*, 47:5096, 1993.
8. D. B. Leinweber. In T. Draper, S. Gottlieb, A. Soni, and D. Toussaint, editors, *Lattice '93*, Proceedings of the International Symposium, **34**, (1994) 383. Dallas, TX, 1993, Nucl. Phys. B (Proc. Suppl. ).
9. D. B. Leinweber. *Nucl. Phys.* , A585:341, 1995.
10. D. B. Leinweber. In preparation, 1998.
11. S. J. Dong, K. F. Liu, and A. G. Williams. Preprint UK-97-23, hep-ph/9712438, 1997.